Int. J. Mol. Sci. **2003**, *4*, 379-407

International Journal of
Molecular Sciences
ISSN 1422-0067

www.mdpi.org/ijms/

Theoretical Calculation of Absolute Radii of Atoms and Ions. Part 2. The Ionic Radii

Dulal C. Ghosh* **and Raka Biswas**

Department of Chemistry, University of Kalyani, Kalyani – 741235, India.
E-mail: dulal@klyuniv.ernet.in
*Author to whom correspondence should be addressed.

Received: 9 May 2003 / Accepted: 12 May 2003 / Published: 31 May 2003

Abstract: The theoretical method of determination of absolute atomic size, discussed in Int. J. Mol. Sci. 2002, 3, 87-113, is exploited to calculate absolute radii of the ions whose experimental radii are published by Shanon. The computed radii are found to reproduce the expected periodic variation of size in periods and in groups and nicely reproduce the d-block and f-block contractions in the respective series. It is pointed out that experimental radii of d and f block transition metal ions make erroneous and misleading representation of the size behaviour of the respective series. A detailed comparative study of the crystal radii vis-à-vis the theoretical radii is reported. A rationale of the double hump curve of the experimental radii of 3 d-block transition metal ions is put forward in terms of the crystal field theory and Jahn-Teller distortion. The theoretical radii are exploited to calculate the diamagnetic susceptibility, polarizability and chemical hardness of the ions and compared with available experimental data. The fact of good agreement between the experimental and computed global hardness of ions and correct demonstration of d-block and f-block contraction by the computed radii are used as benchmark to test the validity of the values of the computed theoretical radii of the ions as their representative sizes. It is concluded that the theoretically computed radii of ions are visualizable size representation of ions and can be used as their absolute radii at the respective oxidation states.

Keywords: Crystal radii, Absolute radii, Chemical hardness, Polarizability.

Introduction

The concept of size of atoms and ions is very useful in understanding, explaining, correlating, predicting, and even calculating many size dependent physico-chemical properties of atoms and ions. The properties like the polarizability, electronegativity, global hardness and diamagnetic susceptibility of atoms and ions can be calculated if the sizes of atoms and ions are available. The shell structure of atoms and ions is established unequivocally by theoretical calculations and experimental verification [1]. The sizes of atoms and ions will be determined by the fundamental laws governing the gradual filing up of their shells and sub-shells by electrons followed by the physical process of inter penetration of charge clouds and the mutual shielding. The periodic trend of size variation is already set out in the chemical literature [2].

A vast array of data labeled as metallic radii, ionic radii, covalent radii and van der Waal radii is found to appear in chemical literature and such radii are tacitly posed as the size of the atoms and ions [3-17]. These are all experimental radii determined by crystallographers with the only significance that when such atomic and ionic radii are added they reproduce the minimum distance of separation between atoms and ions in their crystal lattices. Such approximate additivity of atomic and ionic radii was noted by several crystal chemists like Goldschmidt [18], Zachariasen [19] and Bragg [20]. But such experimental atomic and ionic radii depend upon various factors, like crystal type, its allotropic modification, co-ordination number, temperature etc. Even for a particular ion of particular oxidation state, there is an array of ionic radii for several co-ordination numbers [5]. How ever the size data referred to above are not the absolute sizes of atoms and ions and the experimental [21-22] determination of absolute radii of atoms and ions has not been possible. However, various theoretical methods have been proposed to determine the absolute and covalent radii [4, 6-11]. We [23] have calculated the absolute radii of atoms of 103 elements of the periodic table using the suggestion of Slater [4] that the theoretical radii of an atom or ion is the principal maximum of the radial charge density distribution function. Following the same method [4, 23] we have calculated the absolute radii of all the ions whose radii are published by Shanon [5(b)].

Methods of Computation

The radial charge density distribution function is defined [12, 24, 25] as $4\pi r^2R^2$ or simply r^2R^2, where R is the radial part of the one-electron function. According to Slater [4], theoretical atomic or ionic radius is the principal maximum of the radial charge density distribution function of the outer most electron of the atom or ion. Conveniently, the Slater's analytical form of the radial part of one-electron function [23, 26] is exploited to calculate the radii as follows:

Radial charge density distribution function $\rho(r)$ is given by

$$\rho\,(r) = 4\pi r^2R^2 \qquad (1)$$

Now in terms of Slater's analytical form of the radial part of the one-electron function [26], the radial charge density distribution function can be written as [23]

$$\rho(r) = 4\pi r^2(2\xi)^{2n+1}[(2n)!]^{-1} r^{2n-2}\exp(-2\xi r)$$
$$= 4\pi r^{2n}(2\xi)^{2n+1}[(2n)!]^{-1}\exp(-2\xi r) \quad (2)$$

where n is the principal quantum number of the electron and ξ is the orbital exponent.

Differentiating $\rho(r)$ with respect to r and equating the result with zero, we get the maximum of the radial charge density distribution function, the theoretical radii of atom or ion.

$$d\rho/dr = [4\pi(2\xi)^{2n+1}[(2n)!]^{-1}\exp(-2\xi r)][2nr^{2n-1} - 2\xi r^{2n}]$$

Equating the right hand side of the above equation equal to zero and replacing r by r_{max} we obtain,

$$(nr_{max}^{2n-1} - \xi r_{max}^{2n}) = 0$$

According to definition, the r_{max} is the atomic or ionic radii and it follows from above equation that the atomic or ionic radii r

$$r = r_{max} = n/\xi \quad (3)$$

From the above relation we obtain the formula for computing the theoretical atomic or ionic radii, r. The orbital exponent ξ is obtained by the relation

$$\xi = (Z - S)/n^* = Z^*/n^* \quad (4)$$

where Z is the nuclear charge, S is the screening constant, Z^* is the effective nuclear charge and n^* is the effective principal quantum number. The screening constants, S, for any electron configuration may be calculated from Slater's empirical rules [26] and are also available in any standard text book of inorganic and physical chemistry. The values of n^* for principal quantum number up to 6, and Z^* for about 26 elements are published by Pople [27]. For the rest of the atoms with principal quantum number 7, the n^* value is calculated by simple method of extrapolation and the value is approximately 4.3 [23]. The electron configurations of the ions are generated from the corresponding atomic electron configuration by removing the requisite number of electrons adiabatically from their ground state electronic configurations published by Shriver and Atkins [28]. The calculated ionic radii and those of Shanon [5(b)] are tabulated side by side in Table 1. A comparative study of theoretical ionic radii and Shanon's experimental ionic radii is furnished. But while citing Shandon's data, we have used the golden rule of mean wherever more than one value is cited for the same ion under different coordination number. Shanon [5] has published several radii of the same ion for its different coordination number and we have taken the mean of the crystal radii of each ion. The computed ionic sizes are used to calculate the size dependent physical properties of ions, viz. diamagnetic susceptibility, polarizability, and global hardness according to the algorithm stated below.

Table 1. Computed (a) and Shanon's (b) radii, r, (A^0) of ions.

Ion	(a) Radii	(b) Radii	Ion	(a) Radii	(b) Radii
Ac+3	1.1853408	1.12	Cr+3	0.4535743	0.615
Ag+1	0.6001315	1.061	Cr+4	0.4389429	0.48
Ag+2	0.5844564	0.865	Cr+5	0.4252259	0.468
Ag+3	0.5695793	0.71	Cr+6	0.3735318	0.35
Al+3	0.2391729	0.468	Cs+1	1.1441514	1.788
Am+2	1.5338261	1.26	Cu+1	0.3649448	0.61
Am+3	1.4597793	1.032	Cu+2	0.3554127	0.63
Am+4	1.3925526	0.9	Cu+3	0.3463658	0.54
As+3	1.0655396	0.58	Dy+2	0.8849397	1.13
As+5	0.2793273	0.3975	Dy+3	0.8512735	0.998
At+7	0.5555591	0.62	Er+3	0.7458777	0.975
Au+1	0.6243894	1.37	Eu+2	1.1350313	1.254
Au+3	0.5996261	0.765	Eu+3	1.0802367	1.036
Au+5	0.5879667	0.57	F-1	0.4364289	1.306
B+3	0.1125894	0.13	F+7	0.0608241	0.08
Ba+2	1.0325268	1.474	Fe+2	0.4159415	0.716
Be+2	0.1430189	0.293	Fe+3	0.4036042	0.609
Bi+3	1.8142971	1.053	Fe+4	0.3919778	0.585
Bi+5	0.6207273	0.76	Fe+6	0.3706249	0.25
Bk+3	1.2378246	0.96	Fr+1	1.4416307	1.8
Bk+4	1.1891461	0.88	Ga+3	0.3164472	0.547
Br-1	1.0802367	1.96	Gd+3	0.9913565	1.024
Br+3	0.9054007	0.59	Ge+2	1.2333411	0.73
Br+5	0.8376167	0.31	Ge+4	0.2967308	0.46
Br+7	0.2500016	0.32	Hf+4	0.5822837	0.72
C+4	0.0928368		Hg+1	2.8372519	1.08
Ca+2	0.5442891	1.155	Hg+2	0.7532669	0.9525
Cd+2	0.5574175	1.007	Ho+3	0.7950981	1.027
Ce+3	1.957929	1.168	I-1	1.4597793	2.2
Ce+4	0.863951	1.012	I+5	1.1319144	0.695
Cf+3	1.1503696	0.95	I+7	0.4111137	0.475
Cf+4	1.1082094	0.87	In+3	0.5203798	0.78
Cl-1	0.8282661	1.81	Ir+3	0.6473028	0.68
Cl+5	0.6066917	0.12	Ir+4	0.6337365	0.625
Cl+7	0.1647222	0.175	Ir+5	0.6207273	0.57
Cm+3	1.3396709	0.97	K+1	0.61452	1.5
Cm+4	1.2828364	0.9	La+3	0.9407467	1.189
Co+2	0.3935975	0.709	Li+1	0.1959889	0.757
Co+3	0.3825325	0.578	Lu+3	0.6290535	0.957
Co+4	0.3720727	0.465	Mg+2	0.2696408	0.71
Cr+2	0.4692148	0.765	Mn+2	0.440975	0.795

Table 1. Continued

Ion	(a) Radii	(b) Radii	Ion	(a) Radii	(b) Radii
Mn+3	0.4271327	0.602	Pd+1	0.63159	0.59
Mn+4	0.414133	0.46	Pd+2	0.6142522	0.75
Mn+5	0.4019013	0.33	Pd+3	0.5978409	0.76
Mn+6	0.3903713	0.255	Pd+4	0.5822837	0.615
Mn+7	0.3463658	0.355	Pm+3	1.3162548	1.069
Mo+3	0.7458777	0.69	Po+4	1.597016	1.01
Mo+4	0.7218171	0.65	Po+6	0.586338	0.67
Mo+5	0.6992604	0.535	Pr+3	1.68424	1.098
Mo+6	0.5495941	0.5575	Pr+4	1.5663432	0.905
N-3	0.7426947	1.46	Pt+2	0.6356396	0.7
N+3	0.4276121	0.16	Pt+4	0.6099942	0.625
N+5	0.0789806		Pt+5	0.5979322	0.57
Na+1	0.3090044	1.134	Pu+3	1.6035455	1
Nb+3	0.7950981	0.72	Pu+4	1.5227914	0.91
Nb+4	0.7678153	0.735	Pu+5	1.4497808	0.74
Nb+5	0.5910729	0.638	Pu+6	1.383451	0.71
Nd+2	1.5821648	1.32	Ra+2	1.3009838	1.59
Nd+3	1.4776823	1.131	Rb+1	0.846672	1.652
Ni+2	0.3735318	0.59	Re+4	0.6872338	0.63
Ni+3	0.3635519	0.58	Re+5	0.6719619	0.58
Ni+4	0.3540914	0.48	Re+6	0.657354	0.55
No+2	0.9243144	1.1	Re+7	0.4760922	0.455
Np+2	2.381265	1.1	Rh+3	0.6290535	0.665
Np+3	1.7787227	1.01	Rh+4	0.6118528	0.6
Np+4	1.6799048	0.925	Rh+5	0.5955678	0.55
Np+5	1.5914887	0.75	Ru+3	0.6637047	0.68
Np+6	1.5119143	0.72	Ru+4	0.6445857	0.62
Np+7	0.8744317	0.71	Ru+5	0.6265373	0.565
O-2	0.549787	1.382	Ru+7	0.5933118	0.38
Os+4	0.6594019	0.63	Ru+8	0.4819518	0.36
Os+5	0.6453293	0.575	S-2	1.0026379	1.84
Os+6	0.6318448	0.517	S+4	0.6952599	0.37
Os+7	0.6189123	0.525	S+6	0.1786228	0.205
Os+8	0.4488089	0.39	Sb+3	1.4399184	0.707
P+3	0.8141077	0.44	Sb+5	0.4593382	0.6
P+5	0.1950857	0.28	Sc+3	0.4884646	0.808
Pa+3	2.276	1.04	Se-2	1.2530746	1.98
Pa+4	2.11668	0.955	Se+4	0.9379301	0.5
Pa+5	1.0064214	0.88	Se+6	0.2638521	0.35
Pb+2	2.1000132	1.298	Si+4	0.2148914	0.33
Pb+4	0.6594019	0.774	Sm+2	1.2530746	1.27

Table 1. Continued

Ion	(a) Radii	(b) Radii
Sm+3	1.1866236	1.086
Sn+4	0.4879574	1.082
Sr+2	0.7640699	1.293
Ta+3	0.7697018	0.72
Ta+4	0.7505957	0.68
Ta+5	0.5419873	0.69
Tb+3	0.9159902	1.009
Tb+4	0.8799681	0.82
Tc+4	0.6810188	0.645
Tc+5	0.6609043	0.6
Tc+7	0.5135551	0.465
Te-2	1.693344	2.21
Te+4	1.2674731	0.717
Te+6	0.4338901	0.495
Th+4	1.0885783	1.1
Ti+2	0.538139	0.86
Ti+3	0.5176663	0.67
Ti+4	0.443026	0.569
Tl+1	2.4925391	1.597
Tl+3	0.7032159	0.865
Tm+2	0.7251589	1.06
Tm+3	0.7023961	0.975
U+3	1.9968679	1.025
U+4	1.8731681	1.012
U+5	1.7639	0.8
U+6	0.9357954	0.674
V+2	0.5013189	0.79
V+3	0.4835056	0.64
V+4	0.4669147	0.61
V+5	0.4053217	0.452
W+4	0.7175186	0.66
W+5	0.7008874	0.62
W+6	0.5069072	0.51
Xe+8	0.3906093	0.44
Y+3	0.6961525	0.988
Yb+2	0.6839927	1.08
Yb+3	0.6637047	0.955
Zn+2	0.3389701	0.73
Zr+4	0.6393238	0.747

Diamagnetic susceptibility (χ_{dia})

Using the formula modified by Purcell [29], we have calculated the molar diamagnetic susceptibility of some diamagnetic ions for which experimental diamagnetic susceptibility values are available.

$$\chi_{dia} = -1.888 \times 10^{10} \Sigma_n \, , \langle r^2 \rangle_{av} \quad (5)$$

where, $\langle r^2 \rangle_{av}$ is the mean square of all of the actual orbital radii and Σ_n implies the summation for all n electrons present in the ion. We have calculated the $\langle r^2 \rangle_{av}$ of as many as 16 diamagnetic ions by calculating the radii of each orbital and then evaluated the diamagnetic susceptibility using eqn.(5). The calculated molar diamagnetic susceptibilities of the ions are shown in Table 2.

Polarizability (α)

Polarizability is a very important size dependent physico-chemical property of atoms and ions. According to Pearson [30, 31] polarizability of atoms and ions means the ease of deforming the valence electron cloud of the chemical species. The static electric dipole polarizability describes the linear response of the electron cloud of a chemical species to an external field much smaller than what would be needed to ionize the system**.** It has been shown by Politzer *et al.* [32] that the polarizability, α, of a conducting sphere of radius r is given by:

$$\alpha = r^3 \quad (6)$$

But it is suggested that, due to inhomogeneity of the electron cloud, the actual formula should be

Table 2. Diamagnetic Susceptibility, χ_{dia}, of ions

Ion	Diamagnetic Susceptibility x 10^{-6} cc
Li+1	-0.145
Na+1	-0.924
K+1	-4.5162
Rb+1	-13.3056
Cs+1	-26.4925
Tl+1	-169.872
Hg+2	-18.096
Mg+2	-1.504
Zn+2	-2.1476
Pb+2	-122.992
Ca+2	-3.564
F-1	-1.833
Cl-1	-8.0892
Br-1	-20.9736
I-1	-47.2716
O-2	-2.898

$$\alpha = Kr^3 \quad (7)$$

where K is he proportionality constant. Several values of K were proposed by several groups [22, 33]. However, we have found that K= 4.5 is more appropriate and effective [23] and have computed the polarizability of all the ions through the eqn.(7) using K= 4.5. The computed polarizability of the ions is shown in Table 3.

Table 3. Computed Polarizability, α, and Global hardness, η, of ions.

Ion	Atomic Polarizability $\times 10^{-24}$ cc	Global hardness, eV	Ion	Atomic Polarizability $\times 10^{-24}$ cc	Global hardness, eV
Ac+3	7.494492229	6.066619183	Cl-1	2.556949512	8.68200612
Ag+1	0.972639202	11.9823927	Cl+5	1.004885817	11.85282575
Ag+2	0.898398276	12.30375955	Cl+7	0.020112625	43.65539164
Ag+3	0.831524807	12.62512641	Cm+3	10.81949204	5.367744653
Al+3	0.061567047	30.06616467	Cm+4	9.500058945	5.605556125
Am+2	16.23831169	4.688283305	Co+2	0.274390819	18.2699607
Am+3	13.99826226	4.926094777	Co+3	0.25189389	18.79843064
Am+4	12.15198903	5.163906249	Co+4	0.231790578	19.32690058
As+3	5.44403975	6.748703935	Cr+2	0.464865761	15.32562819
As+5	0.098073695	25.74403554	Cr+3	0.41991152	15.85409813
At+7	0.77161952	12.94373869	Cr+4	0.380571684	16.38256807
Au+1	1.095415894	11.51686986	Cr+5	0.345996431	16.91103801
Au+3	0.970183795	11.9924928	Cr+6	0.234528234	19.25140487
Au+5	0.914683048	12.23030427	Cs+1	6.740047348	6.285017474
B+3	0.006422507	63.86936676	Cu+1	0.218722848	19.70437911
Ba+2	4.953549982	6.964478822	Cu+2	0.202027873	20.23284904
Be+2	0.013164155	50.28013979	Cu+3	0.18698966	20.76131898
Bi+3	26.8743373	3.963524533	Dy+2	3.118555609	8.125990452
Bi+5	1.076254538	11.58481599	Dy+3	2.776002307	8.447357306
Bk+3	8.534730292	5.80939453	Er+3	1.867305634	9.641005621
Bk+4	7.566902284	6.047206002	Eu+2	6.580153618	6.335517979
Br-1	5.672431827	6.656884833	Eu+3	5.672431827	6.656884833
Br+3	3.339911679	7.94235225	F-1	0.374070032	16.4769377
Br+5	2.644529842	8.585085958	F+7	0.001012606	118.2262746
Br+7	0.070313829	28.76386375	Fe+2	0.323824145	17.28851653
C+4	0.003600589	77.45859373	Fe+3	0.295855512	17.81698647
Ca+2	0.725607107	13.21174844	Fe+4	0.271017199	18.34545641
Cd+2	0.779389108	12.90058371	Fe+6	0.229095366	19.40239629
Ce+3	33.77562007	3.672764046	Fr+1	13.48262895	4.988109106
Ce+4	2.901882875	8.323401519	Ga+3	0.142598904	22.72420732
Cf+3	6.850537746	6.251044406	Gd+3	4.384317843	7.253708991
Cf+4	6.124604243	6.488855878	Ge+2	8.442326205	5.830512923

Table 3. Continued

Ion	Atomic Polarizability $\times 10^{-24}$ cc	Global hardness, eV	Ion	Atomic Polarizability $\times 10^{-24}$ cc	Global hardness, eV
Ge+4	0.1175711	24.234121	Np+4	21.333715	4.280606496
Hf+4	0.8884162	12.349669	Np+5	18.139412	4.518417968
Hg+1	102.77943	2.5344987	Np+6	15.552279	4.75622944
Hg+2	1.9233538	9.5464319	Np+7	3.0087787	8.223639337
Ho+3	2.2619063	9.0441815	O-2	0.7478181	13.07963096
I-1	13.998262	4.9260948	Os+4	1.2902178	10.90535464
I+5	6.5260938	6.3529636	Os+5	1.2093628	11.14316612
I+7	0.3126787	17.491539	Os+6	1.1351251	11.38097759
In+3	0.6341234	13.818775	Os+7	1.0668413	11.61878906
Ir+3	1.2204918	11.109193	Os+8	0.406815	16.02243315
Ir+4	1.1453514	11.347005	P+3	2.4280526	8.832997531
Ir+5	1.0762545	11.584816	P+5	0.033411	36.86077816
K+1	1.0442887	11.701834	Pa+3	53.055363	3.159495271
La+3	3.7465418	7.6439402	Pa+4	42.675452	3.397306743
Li+1	0.0338771	36.690913	Pa+5	4.5872472	7.14512926
Lu+3	1.1201476	11.431478	Pb+2	41.675288	3.424269495
Mg+2	0.0882204	26.668858	Pb+4	1.2902178	10.90535464
Mn+2	0.3858819	16.307072	Pd+1	1.1337525	11.38556854
Mn+3	0.350672	16.835542	Pd+2	1.0429242	11.7069354
Mn+4	0.3196187	17.364012	Pd+3	0.9615446	12.02830225
Mn+5	0.2921263	17.892482	Pd+4	0.8884162	12.3496691
Mn+6	0.2676987	18.420952	Pm+3	10.262009	5.463236519
Mn+7	0.1869897	20.761319	Po+4	18.329067	4.502779572
Mo+3	1.8673056	9.6410056	Po+6	0.9071028	12.26427734
Mo+4	1.6923652	9.9623725	Pr+3	21.499306	4.269588204
Mo+5	1.5386124	10.283739	Pr+4	17.293117	4.590955058
Mo+6	0.7470312	13.084222	Pt+2	1.1557008	11.31303145
N-3	1.8435017	9.6823242	Pt+4	1.0213855	11.7886544
N+3	0.351854	16.816668	Pt+5	0.9619851	12.02646587
N+5	0.002217	91.047821	Pu+3	18.554803	4.4844449
Na+1	0.132772	23.271551	Pu+4	15.89036	4.722256372
Nb+3	2.2619063	9.0441815	Pu+5	13.712592	4.960067844
Nb+4	2.0369614	9.3655483	Pu+6	11.915269	5.197879316
Nb+5	0.9292566	12.166031	Ra+2	9.9089625	5.527364145
Nd+2	17.822462	4.5450455	Rb+1	2.7312289	8.493266857
Nd+3	14.519635	4.8664124	Re+4	1.4605821	10.46370477
Ni+2	0.2345282	19.251405	Re+5	1.3653578	10.70151624
Ni+3	0.2162279	19.779875	Re+6	1.2782344	10.93932771
Ni+4	0.1997831	20.308345	Re+7	0.4856077	15.10424214
No+2	3.5536257	7.7798324	Rh+3	1.1201476	11.43147809
Np+2	60.762509	3.0198282	Rh+4	1.0307501	11.75284495
Np+3	25.324288	4.042795	Rh+5	0.950618	12.0742118

Table 3. Continued

Ion	Atomic Polarizability $\times 10^{-24}$ cc	Global hardness, eV	Ion	Atomic Polarizability $\times 10^{-24}$ cc	Global hardness, eV
Ru+3	1.3156406	10.834654	Te+4	9.1628108	5.6735023
Ru+4	1.2051871	11.156021	Te+6	0.3675798	16.573348
Ru+5	1.1067595	11.477388	Th+4	5.8048569	6.6058742
Ru+7	0.9398564	12.120121	Ti+2	0.7012871	13.36274
Ru+8	0.5037595	14.920604	Ti+3	0.6242542	13.89121
S-2	4.5357056	7.172092	Ti+4	0.3912914	16.231577
S+4	1.5123558	10.342912	Tl+1	69.68486	2.8850145
S+6	0.0256462	40.258085	Tl+3	1.5648714	10.225893
Sb+3	13.434643	4.9940409	Tm+2	1.7159793	9.9164629
Sb+5	0.4361242	15.655157	Tm+3	1.5594042	10.23783
Sc+3	0.5244594	14.721663	U+3	35.831133	3.6011451
Se-2	8.8540761	5.7386938	U+4	29.576229	3.8389566
Se+4	3.7129908	7.6668949	U+5	24.696442	4.0767681
Se+6	0.0826597	27.25395	U+6	3.6876966	7.6843843
Si+4	0.0446549	33.463471	V+2	0.5669632	14.344184
Sm+2	8.8540761	5.7386938	V+3	0.5086476	14.872654
Sm+3	7.5188513	6.0600607	V+4	0.458063	15.401124
Sn+4	0.5228272	14.736966	V+5	0.2996485	17.741491
Sr+2	2.0072973	9.4114579	W+4	1.6623103	10.022055
Ta+3	2.0520127	9.3425935	W+5	1.5493777	10.259866
Ta+4	1.902965	9.580405	W+6	0.5861353	14.186051
Ta+5	0.7164399	13.26786	Xe+8	0.2681885	18.40973
Tb+3	3.4584775	7.8505331	Y+3	1.5181886	10.329649
Tb+4	3.0662904	8.1719	Yb+2	1.4400144	10.513287
Tc+4	1.4213132	10.559197	Yb+3	1.3156406	10.834654
Tc+5	1.2990571	10.880563	Zn+2	0.1752656	21.214293
Tc+7	0.6095001	14.002413	Zr+4	1.1759126	11.24784
Te-2	21.849832	4.2466334			

Global hardness (η)

The chemical hardness, electronegativity and polarizability are periodic properties of elements [1, 21, 34] and such periodicity is correlated in terms of shell structure of atoms. The chemical hardness of atoms is inversely related to their sizes [1,21,23,34]. We [23] have derived the necessary mathematical relation between the chemical hardness and the radius of the atom

$$\eta = e^2/2R \quad (8)$$

where η is a chemical hardness, e is the electronic charge in e.s.u and R is the radius of atom in cm. The eqn.(8) further vindicates the predicted inverse relationship between the hardness and atomic radius on the basis of shell structure of atoms. Since ions are derived from the atomic electron

configurations and have the shell structures, we assume that the fundamental mathematical relationship between the size and hardness of atoms remains unaltered due to the transition from atom to ion. Hence the chemical hardness of ions is computed by the same formula given by the eqn.(8). We have calculated the chemical hardness of all the ions whose radii are computed and are shown in Table 3.

The Difference Between Shanon's Radii and Theoretical Radii, Δr

$$\Delta r = r_{\text{Shanon}} - r_{\text{theoretical}} \quad (9)$$

The Δr values are calculated through this formula for ions of as many as 14 diverse elements, viz. Cl, Br, I, S, Se, Te, Cr, Mn, Fe, Mo, Np Os, Ru, and Pd in their different oxidation states. Results are shown in Table 4.

Table 4. Difference in experimental (Shanon's) and theoretical radii, Δr, in A^0

Ions	Difference in radii, A^0	Ions	Difference in radii, A^0
S-2	0.8374	Fe+2	0.3001
S+4	-0.3252	Fe+3	0.2054
S+6	0.0264	Fe+4	0.193
Se-2	0.7269	Fe+6	-0.1206
Se+4	-0.4379	Mo+3	-0.0559
Se+6	0.0286	Mo+4	-0.0718
Te-2	0.5167	Mo+5	-0.164
Te+4	-0.5504	Mo+6	0.00789
Te+6	0.0611	Pd+1	-0.0416
Cl-1	0.9817	Pd+2	0.1358
Cl+5	-0.4867	Pd+3	0.1622
Cl+7	0.0103	Pd+4	0.0328
Br-1	0.8798	Ru+3	0.0163
Br+3	-0.3154	Ru+4	-0.0246
Br+5	-0.5276	Ru+5	0.0615
Br+7	0.07	Ru+7	-0.2133
I-1	0.7402	Ru+8	-0.1219
I+5	-0.4369	Os+4	-0.0294
I+7	0.0639	Os+5	-0.068
Cr+2	0.2958	Os+6	-0.1148
Cr+3	0.1614	Os+7	-0.0939
Cr+4	0.0411	Os+8	-0.0588
Cr+5	0.0428	Np+2	-1.2812
Cr+6	-0.0235	Np+3	-0.7687
Mn+2	0.354	Np+4	-0.7549
Mn+3	0.1749	Np+5	-0.8415
Mn+4	0.0459	Np+6	-0.792
Mn+5	-0.0719	Np+7	0.1644
Mn+6	-0.1353		
Mn+7	0.0086		

Results and Discussion

Theoretical Ionic Radii vis-à-vis Experimental Ionic Radii

The nature of the variation of the computed ionic sizes in groups and periods, and a comparative study of the computed sizes vis-à-vis the experimental size of ions can easily be performed from Table 1 and figs. 1 – 9. It is already mentioned that wherever more than one experimental radii of an ion at the same oxidation state are available, we have taken mean of the different values. A look at the Table 1 and figs. 1 – 9 reveals the following general features of the computed sizes of the ions, viz. (i) the expected group trend and horizontal periodic trend of the ionic size are reproduced by the computed sizes of the ions, (ii) the d-block contraction, the lanthanide contraction, and the actinide contraction are distinct in the computed sizes of the respective series (figs. 3,4,5,6,7 respectively), (iii) the profiles of the computed and experimental sizes of anions of group VI and group VII elements run parallel but the experimental sizes of the anions are consistently larger than that of theoretical sizes (figs.8, 9), (iv) the computed size of ions of group I, II and that of first transition series i.e. ions with small positive charge, is always smaller than the experimental size (figs. 1,2,3,4), (v) the profiles of the experimental and theoretical radii of the ions of second transition series and lanthanides (figs.5,6) intersect and cross each other signifying that experimental radii of some ions are larger, some ions are smaller than that of theoretical radii. The intersection of profiles also signifies that experimental and theoretical radii of a few ions are nearly equal, (vi) the expected lanthanide and actinide contractions are distinct in the profile of theoretical radii while the said size contraction is not distinct in the profiles of experimental radii (figs.6 and 7).

We may refer to the curves of the experimental and theoretical radii in figs. 3, 6 and 7 where from it is evident that while the d-block and f-block contractions are nicely reproduced in the profiles of theoretical radii but the experimental radii do not follow the size contraction rule in the series. In fig.3 where the appearance of the curve of the experimental radii of the transition metal ions is anomalous

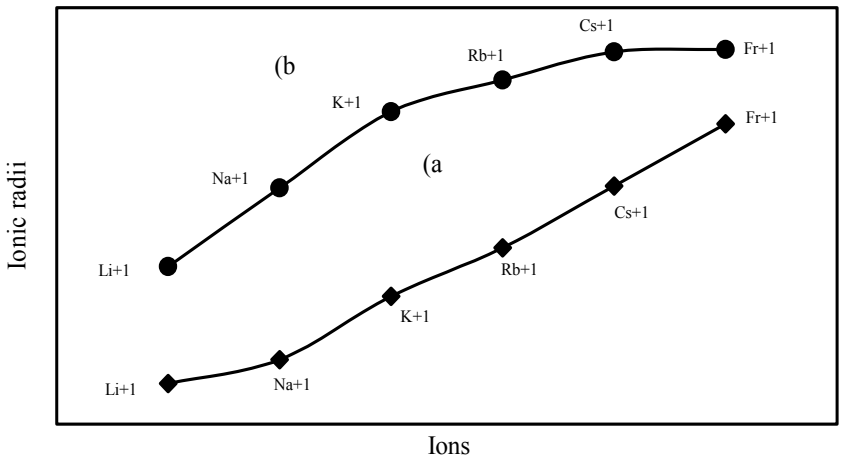

Figure 1. Plot of radii of monopositive ions of Gr-IA elements

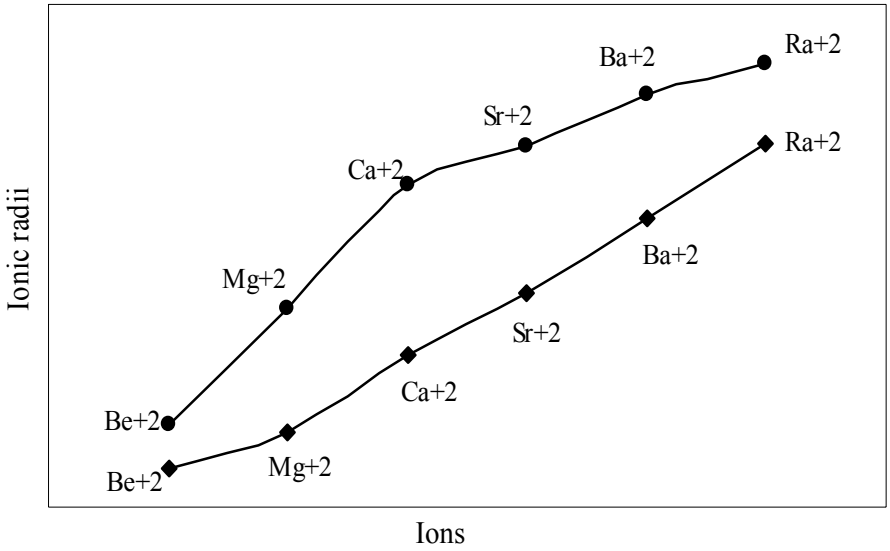

Figure 2. Plot of radii of dipositive ions of Gr-IIA elements

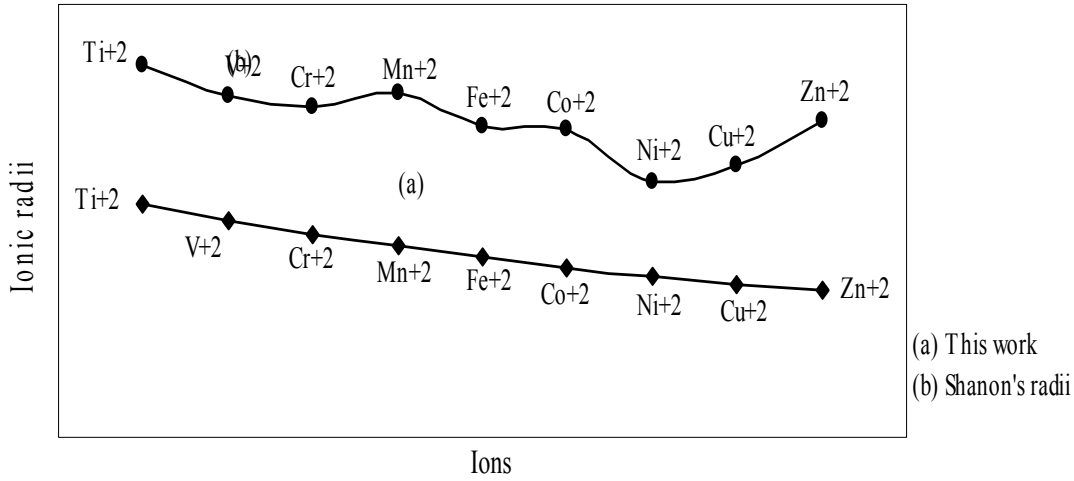

Figure 3. Plot of radii of dipositive ions of first transition series (3d- block) elements

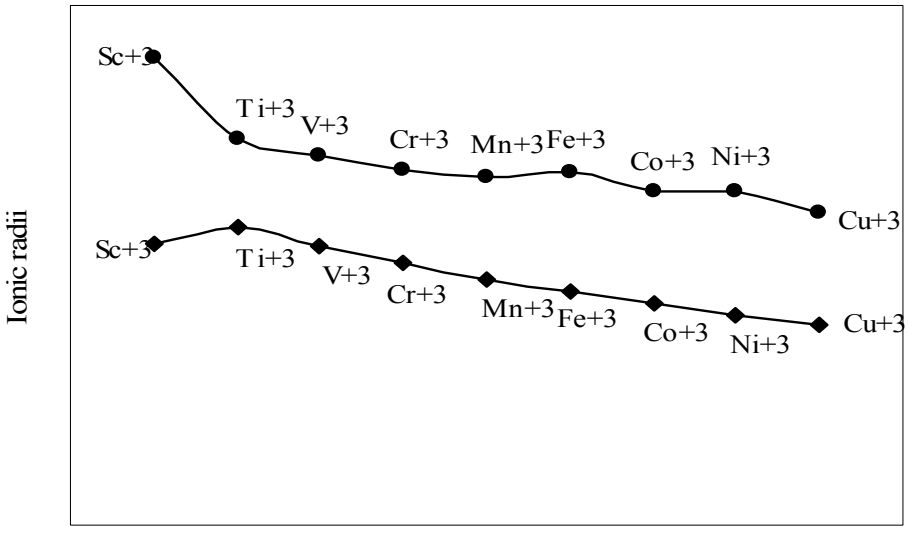

Figure 4. Plot of radii of tripositive ions of first transition series (3d-block) elements

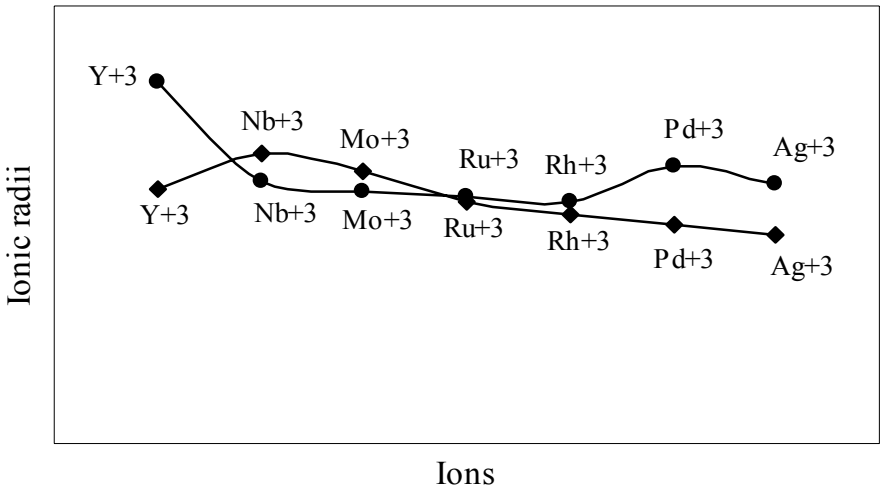

Figure 5. Plot of radii of tripositive ions of second transition series (4d-block) elements

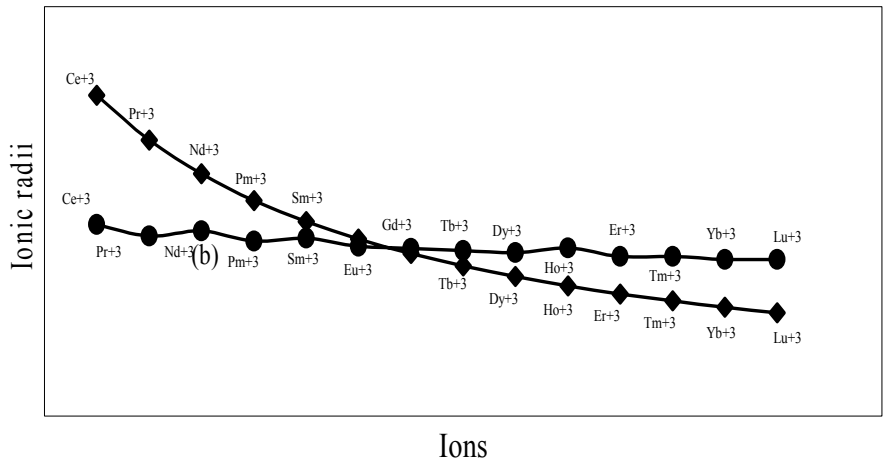

Figure 6. Plot of radii of tripositive ions of lanthanide (4f-block) elements

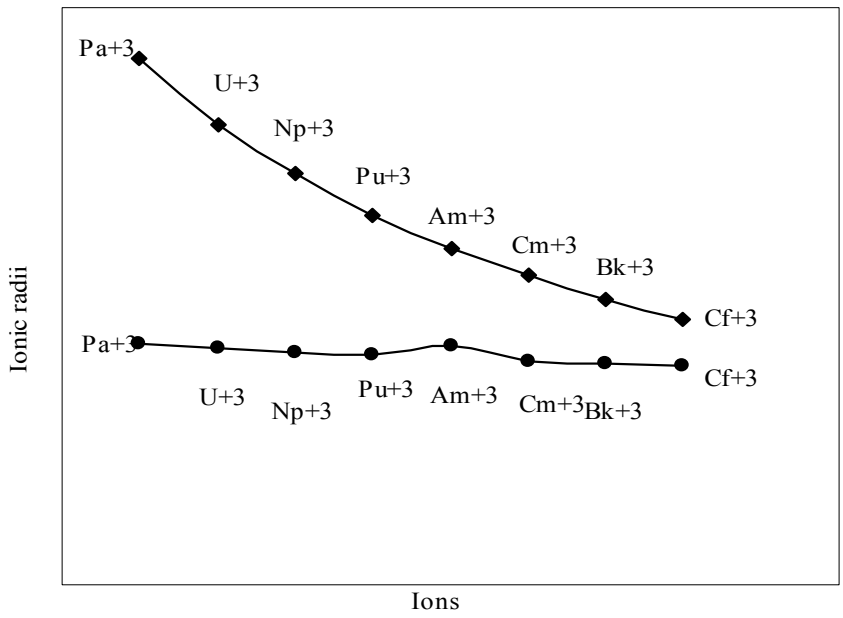

Figure 7. Plot of radii of tripositive ions of actinide (5-f block) elements

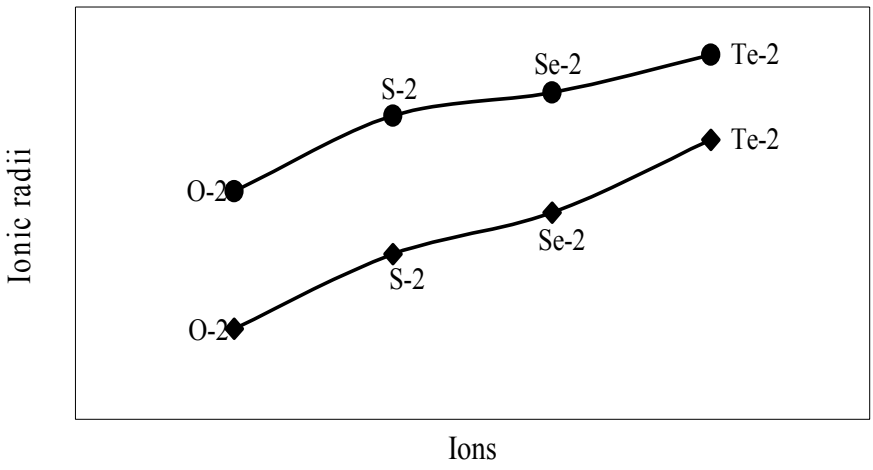

Figure 8. Plot of radii of dinegative ions of Gr-VIB elements.

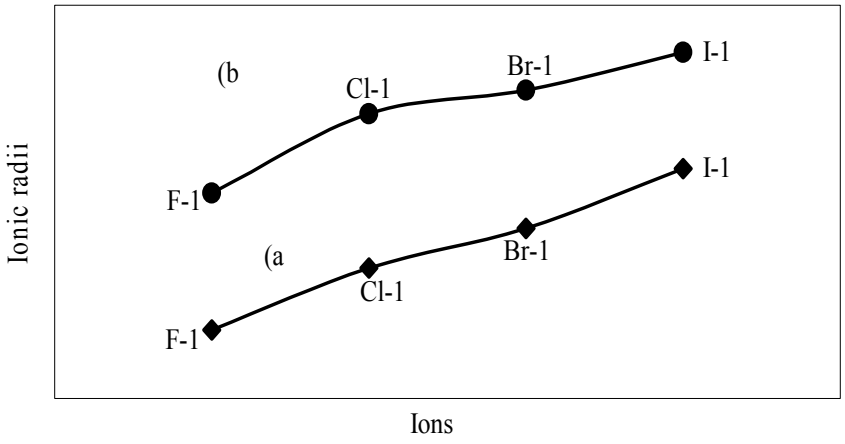

Figure 9. Plot of radii of mononegative ions of Gr-VIIB elements

and double hump type and there is no gradual contraction of experimental ionic radii as a function of atomic number. The profiles of the experimental size of the ions of lanthanide and actinide elements (fig. 6 and 7) show that the expected f-block contraction is missing and radii remain virtually constant with increasing atomic number. On other hand, the profiles of theoretical radii of such series of ions (d- and f-block elements) are smooth and monotone decreasing functions of atomic number. While a rationale of this differential trend of variation of experimental and theoretical radii of the d-block transition metal ions may be put forward in terms of the structural effects of crystal field splitting [35,36], the reason of the near constancy of the experimental sizes of the tripositive ions of the lanthanide actinide elements is not very straightforward.

We may venture to rationalize the profile of the radii of the transition metal ions as follows: The general pattern of variation of size in the series is anomalous and without any general trend. The radii of the transition metal ions are usually estimated by apportioning the internuclear distance between the ions in the crystals of their oxides and halides. The internuclear distance in such compounds should

vary anomalously because of the crystal field splitting of the degeneracy of the d orbitals and structural distortion from Jahn–Teller effect. The charge density distribution around the $d^0(C_a^{+2})$, $d^5(M_n^{+2})$, $d^{10}(Z_n^{+2})$ metal ions having electron configuration $t_{2g}^0\ e_g^0$, $t_{2g}^3\ e_g^3$ and $t_{2g}^6\ e_g^4$ respectively are spherical because all d-orbitals are either unoccupied or equally occupied. It is seen from the profile of the experimental radii that the sizes of other ions are all below the expected curve passing through C_a^{+2}, M_n^{+2}, Z_n^{+2} i.e. have radii smaller than that of C_a^{+2}, M_n^{+2}, Z_n^{+2} ions. The splitting of the degeneracy of the d-orbitals and the Jahn–Teller effect for asymmetric charge distribution conjointly determine the length of metal–ligand bonds of the coordination complexes formed by metal ions with electron configurations d^1– d^4 and d^6– d^9. The electron density distribution in ions of electron configurations d^1– d^4 and d^6– d^9 ions are asymmetric which may lead to Jahn–Teller effect and because of splitting of the degeneracy of the d-orbitals, the electron density is mostly placed in between the axes in t_{2g} orbitals and the ligands approaching along the X, Y, Z axes may be attracted closer to the nucleus compared to the situation in symmetrical distribution of electron density in d^0, d^5, d^{10} ions. As a result, the metal–ligand distance in case of ions with electron configuration d^1– d^4 and d^6– d^9 will be shorter and hence the experimental radii of such ions will be smaller than that of the C_a^{+2}, M_n^{+2}, Z_n^{+2} ions. But under any event, the shielding of one d-electron by another from the nuclear charge is imperfect and there should be a steady contraction in the radii of the d-block transition metal ions and the profile of sizes of such ions as function of atomic number should have a monotone decreasing trend. Thus, it can be safely argued that the double hump curve or the curve of experimental sizes of the ions is not the representative size behaviour of the transition metal ions and the experimental determination of the sizes of the ions of the instant transition metal series creates a wrong and misleading impression regarding the size variation of the ions of the series. We may further claim that the absolute radii and not the experimental radii are the representative sizes of the d-block and f-block transition metal ions.

We have argued that the double hump curve is not the true representative size behaviour of the d-block transition metal ions and the error crops up from the method of measurement of size of such ions. We may put forward the similar argument in case of ions of f-block elements and may be safely concluded that the near constancy of the sizes of the ions of series must be occurring in the method of measurements of the radii of such ions.

Correlation of size behaviour

After rationalizing the size behaviour of the ions of the 3d-block transition metals, we may venture to propose a rationale of above observed relationships between the experimental and theoretical radii of the rest of the ions as below:

The crystal radii are determined by apportioning the X-ray spectrometrically measured closest inter ionic distance between the ions in the solid state. It is quite expected that the ions do not really touch each other and there remains some variable gap between the ions in solid state and hence by the method of determination of crystal radii this gap between the ions is automatically added to the ionic

sizes. The inter ionic distance is bound to decrease with increasing co-valences between the ions, which should increase monotonically with increasing ionic potential which, in turn, increases with the increasing oxidation states of the ions. It may be predicted that the bonding between the ions with high oxidation states should be predominantly covalent than ionic. Thus, it transpires that the experimental or crystal radii of ions with small oxidation states shall be larger than the theoretical or absolute radii and the difference between the absolute radii and experimental radii should decrease steadily with increasing covalency and the physical situation may so change that and the crystal radii of ions with sufficient covalency will be smaller than the absolute radii. It is evident from the radii data in Table 1 and from their profiles in figs. 1-9 that the results are in conformity with the above prediction. Shanon [5(b)] himself referred this aspect of decreasing experimental radii as "covalent shortening". Shanon [5(b)] also pointed out that this effect should be prevalent in compounds with anions less electronegative than O and F i.e. in Cl^{-}, Br^{-}, S^{2-}, Se^{2-}, and in the tetrahedral oxy anions such as VO_4^{3-}, AsO_4^{3-} groups. Shanon had correlated the smaller radii of the cations derived from metallic oxides of Mo^{4+}, Tc^{4+}, Rh^{4+}, Ru^{4+}, Re^{4+}, W^{4+} and Ir^{5+} to the effect of electron delocalization which is only possible through the development of covalency between the cation and anion.

We have made a more critical comparative study of the theoretical versus experimental size variations of ions. For this purpose, we have calculated Δr, the difference of size of an ion in Shanon's determination and the theoretical determination in a particular oxidation state for as many as 14 diverse elements viz. Cl, Br, I, S, Se, Te, Cr, Mn, Fe, Mo, Np Os, Ru and Pd through the eqn. (9). From the Table 4 and figs. 10 – 23 a distinct differential trend of variation of the profiles of Δr for nonmetals and metals is evident. It is evident from figs. 10, 11, 12, 13, 14, and 15 for S, Se, Te, Cl, Br, and I, respectively, that when non-metal atom is negatively charged, its crystal radius is larger than the absolute radius. But as expected, as soon as their oxidation states begin to increase, the experimental radii of such element decrease and the Δr-values decrease. But surprisingly the profiles of Δr take a turn to increase in the highest oxidation states of these elements. This comparative increase in experimental radii of ions at the highest oxidation states must be lying in their method of determination. The rationale of larger value of the crystal radii, compared to the absolute radii, of the anions is already stated above.

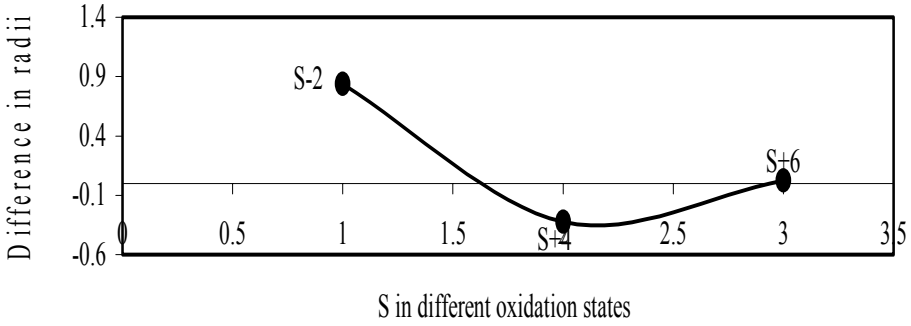

Figure 10. Plot of difference in experimental and theoretical radii of S in different oxidation states

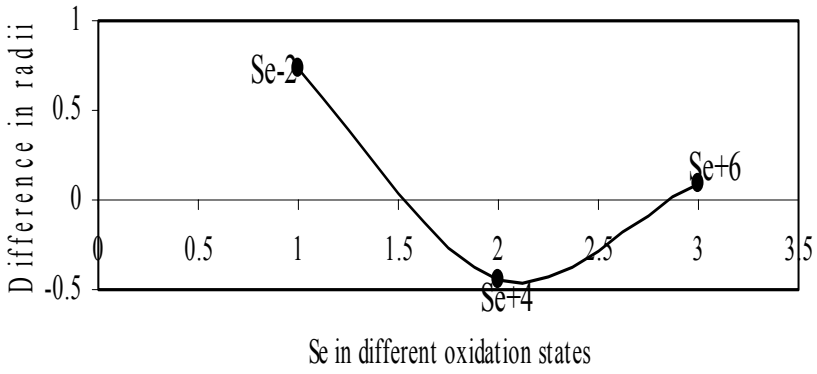

Figure 11. Plot of difference in experimental and theoretical radii of Se in different oxidation states.

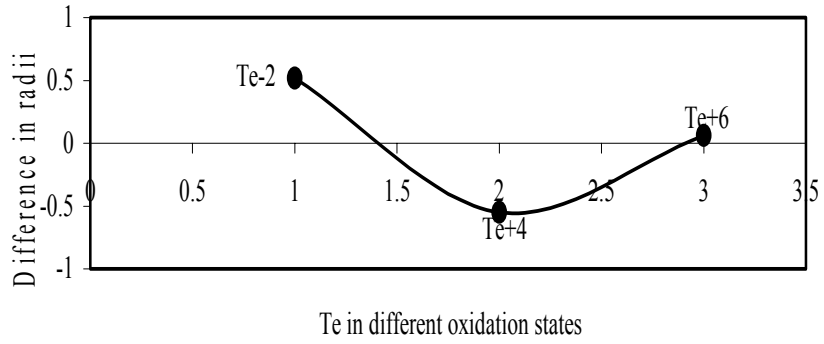

Figure 12. Plot of difference in experimental and theoretical radii of Te in different oxidation states.

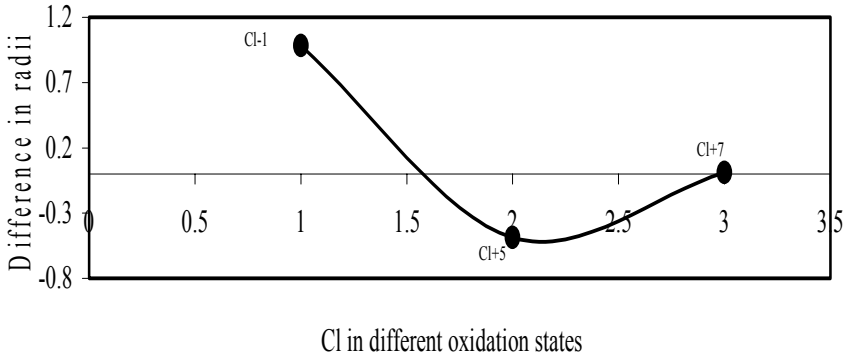

Figure 13. Plot of difference in experimental and theoretical radii of Cl in different oxidation states.

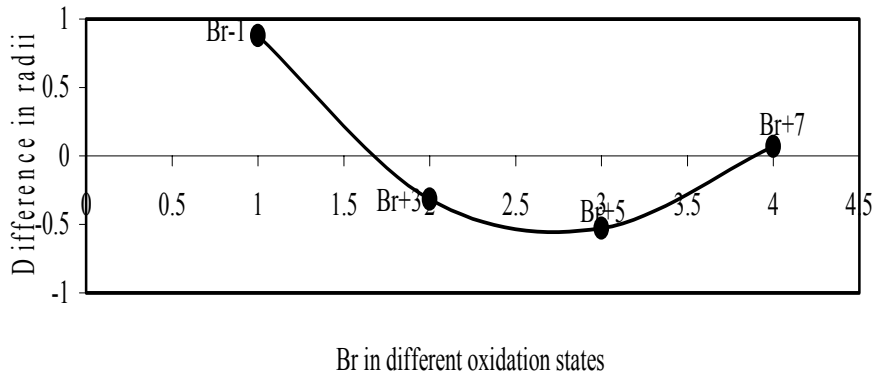

Figure 14. Plot of difference in experimental and theoretical radii of Br in different oxidation states

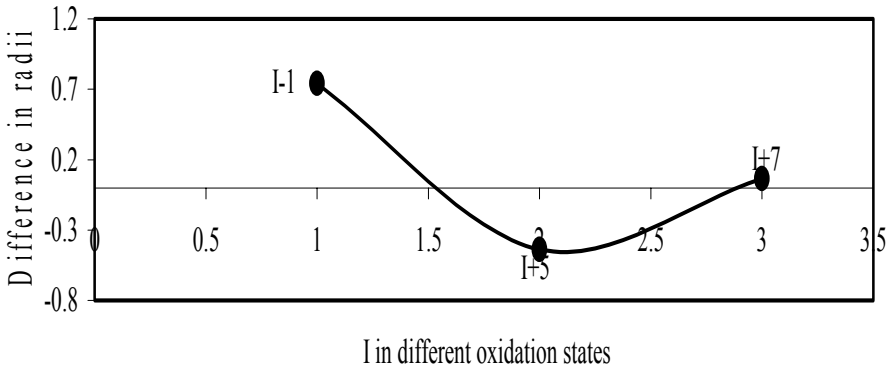

Figure 15. Plot of difference in experimental and theoretical radii of I in different oxidation states.

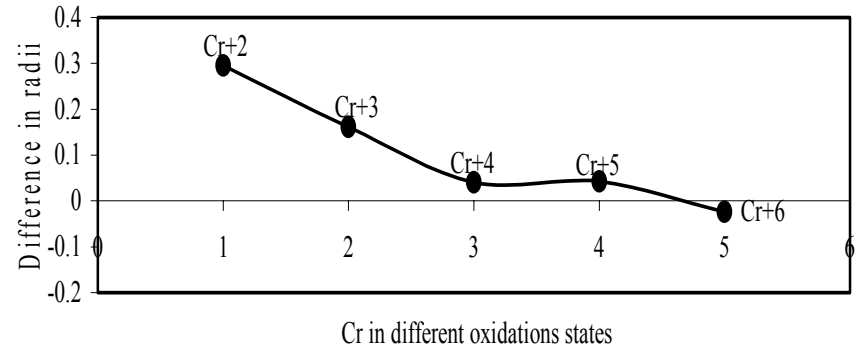

Figure 16. Plot of difference in experimental and theoretical radii of Cr in different oxidation states.

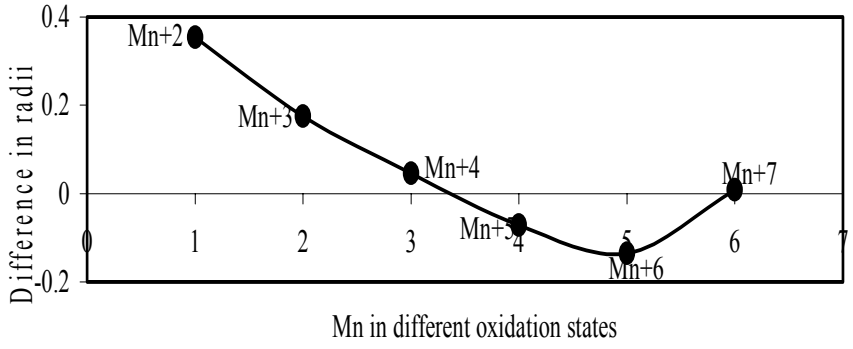

Figure 17. Plot of difference in experimental and theoretical radii of Mn in different oxidation states.

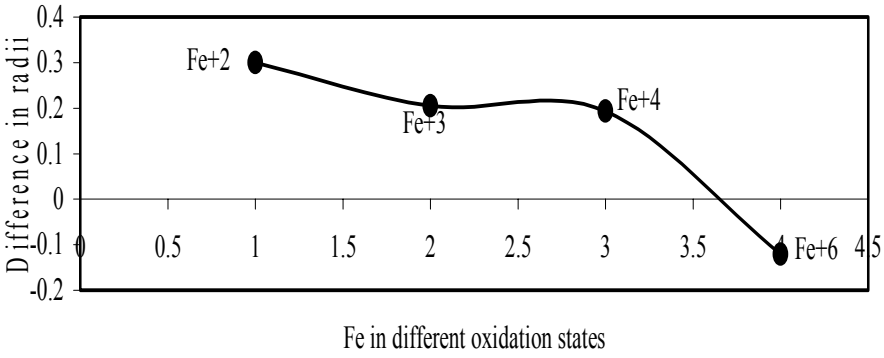

Figure 18. Plot if difference in experimental and theoretical radii of Fe in different oxidation states.

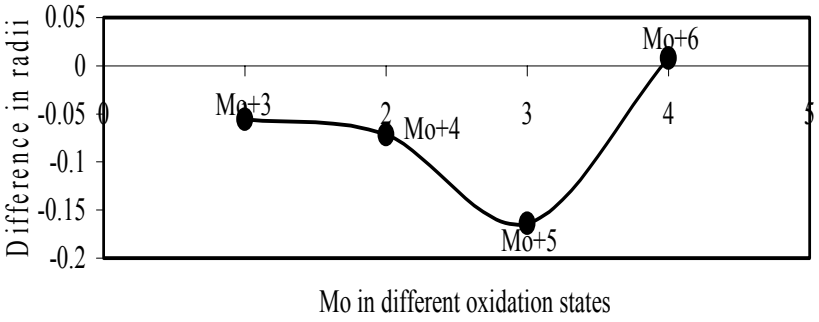

Figure 19. Plot of difference in experimental and theoretical radii of Mo in different oxidation states.

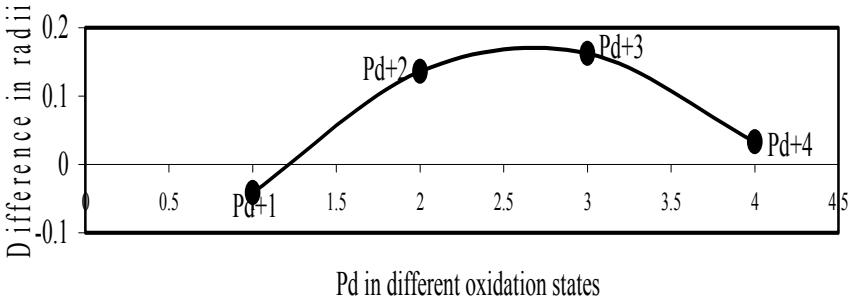

Figure 20. Plot of difference in experimental and theoretical radii of Pd in different oxidation states.

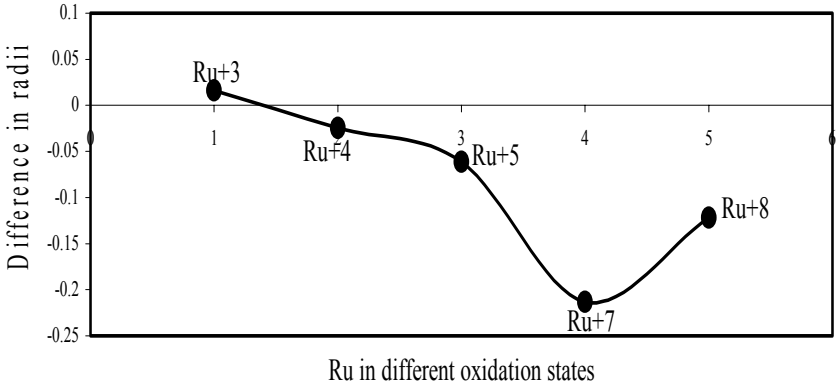

Figure 21. Plot of difference in experimental and theoretical radii of Ru in different oxidation states.

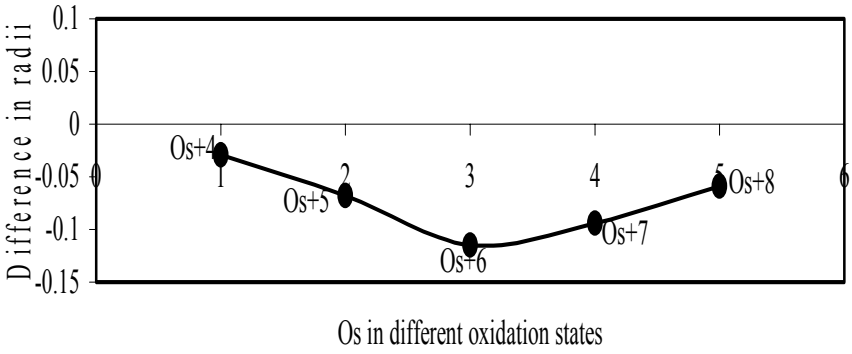

Figure 22. Plot of difference in experimental and theoretical radii of Os in different oxidation states.

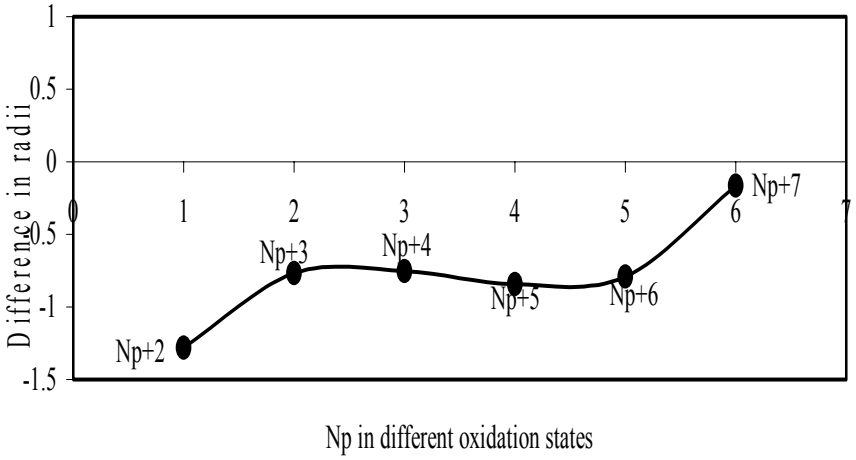

Figure 23. Plot of difference in experimental and theoretical radii of Np in different oxidation states

Now let us consider the cases of metal ions. From the Δr profiles of Cr and Fe (figs. 16, 18 respectively) it is evident that below highest oxidation states i.e. +6, the experimental radii are larger than absolute radii and at the highest oxidation state, the trend is reversed. But in case of Mn, (fig.17), the trend is similar to that of Cr and Fe from +2 to +4 oxidation states and thereafter the trend is reversed and at the highest oxidation state of Mn (i.e Mn +7), the experimental radius is slightly larger than the theoretical radius. Regarding the size variation of Mo, Pd, Ru, Os and Np with increasing oxidation states we have the following general observation. The experimental radii of Mo and Ru (figs. 19 and 21 respectively) are mostly smaller while that of Pd (fig.20) is mostly larger than the theoretical radii. But for Os and Np (figs. 22 and 23) the experimental radii at all the oxidation states are smaller than the theoretical radii.

Thus from the comparative study it transpires that trend of variation of the experimental ionic radii with oxidation states of metals and non-metal are anomalous and no simple correlation and rationalization of such size behaviour can be contemplated. But we have observed, in all cases, that the theoretical radii of ions of a particular element decrease monotonically with increasing oxidation

states. This size behaviour follows from the shell structure of atoms. But it is evident from the above study that this trend is not followed by the available experimental radii in all cases.

Diamagnetic Susceptibility (χ_{dia})

The diamagnetic part of the susceptibility is calculated for as many as 16 typical ions through the formula laid down above and are shown in Table 2. The computed χ_{dia} values are plotted as a function of ionic radii in fig. 24. The computed and the experimental diamagnetic susceptibility values [12, 37] are also plotted in fig. 25 for comparative study. The figure reveals the fact that the trends of both the experimental and theoretical curves are similar. Although the diamagnetic susceptibility is computed through the radii of all the electron shells, the nature of the profiles reveals that the diamagnetic susceptibility is perfectly correlated with variation of ionic radii.

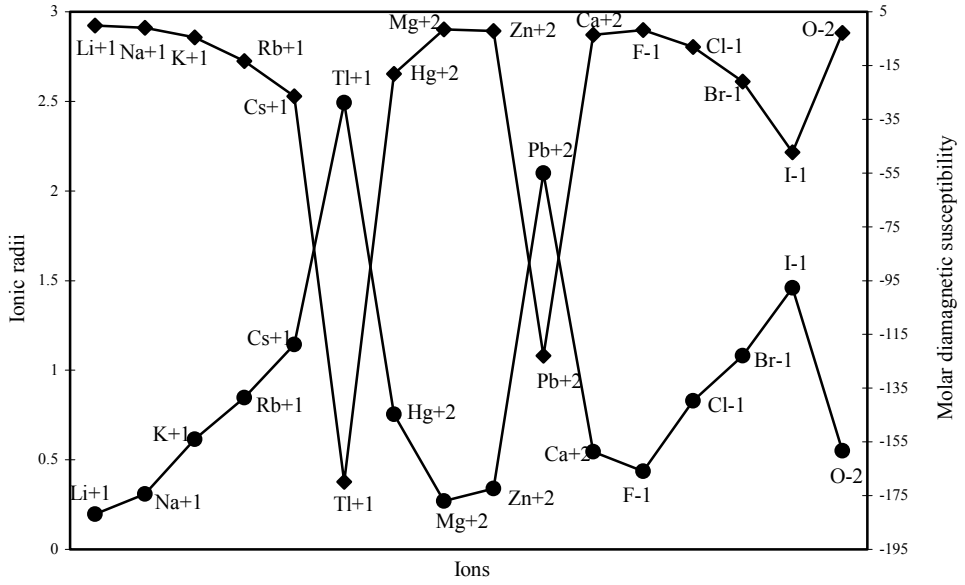

Figure 24. Plot of radii and molar diamagnetic susceptibility of ions

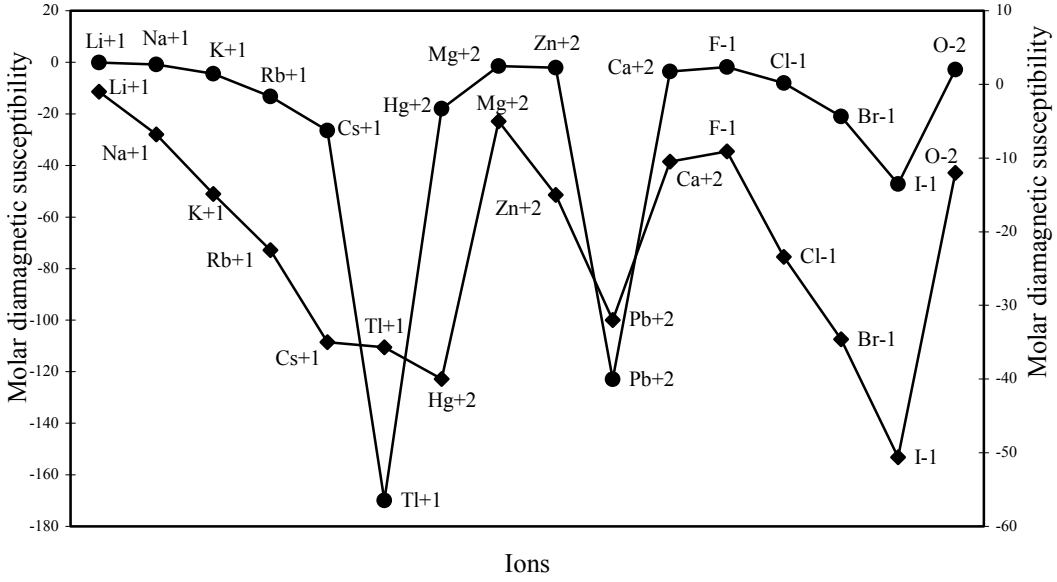

Figure 25. Plot of molar diamagnetic susceptibility of some typical ions.

Polarizability (α) and Global Hardness (η)

The polarizability and global hardness are both size dependent property but are mutually inversely related because of the fact that polarizability is directly related and the hardness is inversely related to size. We have extrapolated the polarizability and hardness of some representative ions in figs. 26 – 29. The natures of the profiles demonstrate that the two properties correlate perfectly with each other. When the hardness increases, the polarizability decreases and when hardness decreases polarizability increases. We could not verify the efficaciousness of the theoretical sizes of ions in terms of computed polarizability because of the fact that there seems to be no report of experimental polarizability of ions and hence there is no possibility of any comparative study of computed and experimental polarizability.

However, we have scope of making a comparative study of the computed hardness vis-à-vis experimental hardness. Pearson [38] published the global hardness of as many as 52 ions computed through ionization potential and electron affinity and they are labeled as "experimental" hardness. Although hardness is not an experimental quantity, such hardness values are labeled as "experimental" probably in view of the fact that their determination relies upon experimental ionization potentials and electron affinities. Table 5 lists the theoretical and experimental hardness of such 52 ions and the values are extrapolated in fig. 30. Table 5 demonstrates that 'experimental' and theoretical hardness of as many as 10 ions are very close. The fig. 30 demonstrates that the two sets of hardness data are close and correlated to each other within a small limit of variation. The qualitative trend of the size

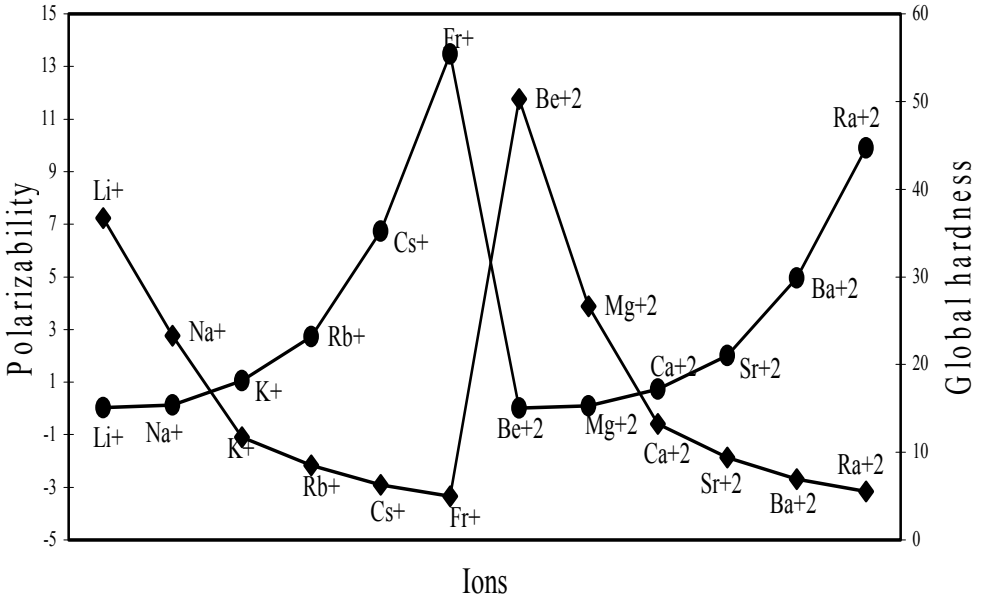

Figure 26. Plot of polarizability and global hardness of ions of Gr-I and Gr-II elements.

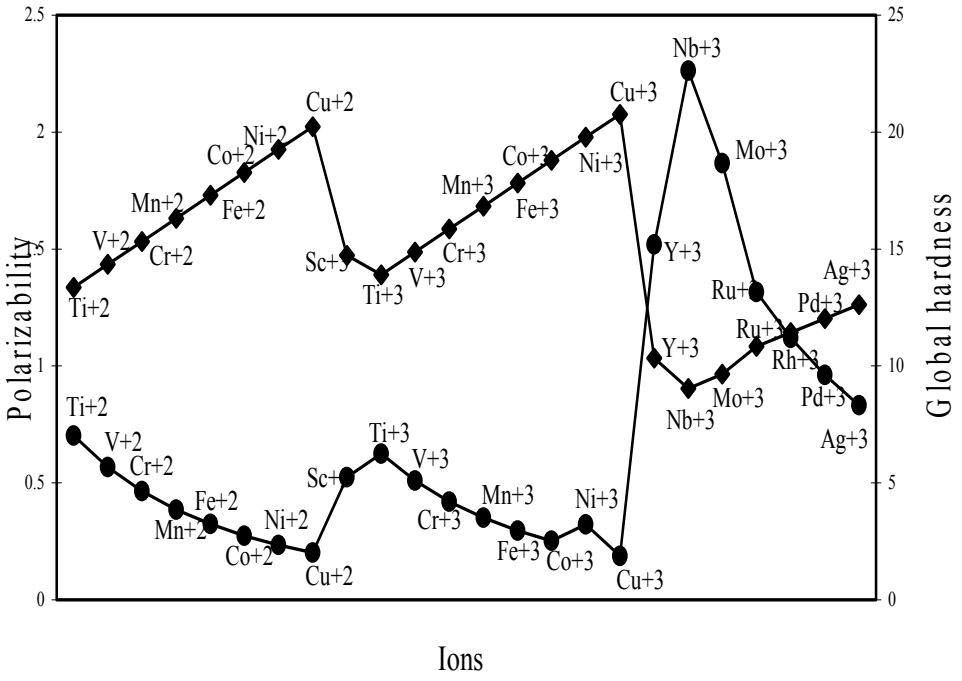

Figure 27. Plot of polarizability and global hardness of some common ions of 1st (3d) and 2nd (4d) transition series elements

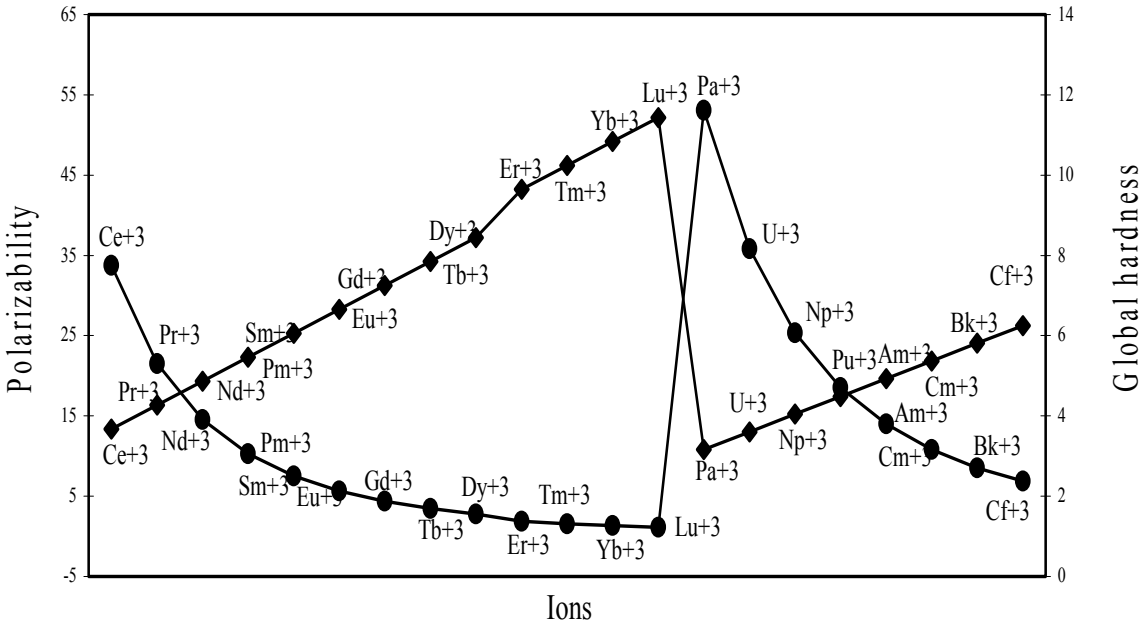

Figure 28. Plot of polarizability and global hardness of ions of elements of lanthanide and actinide series.

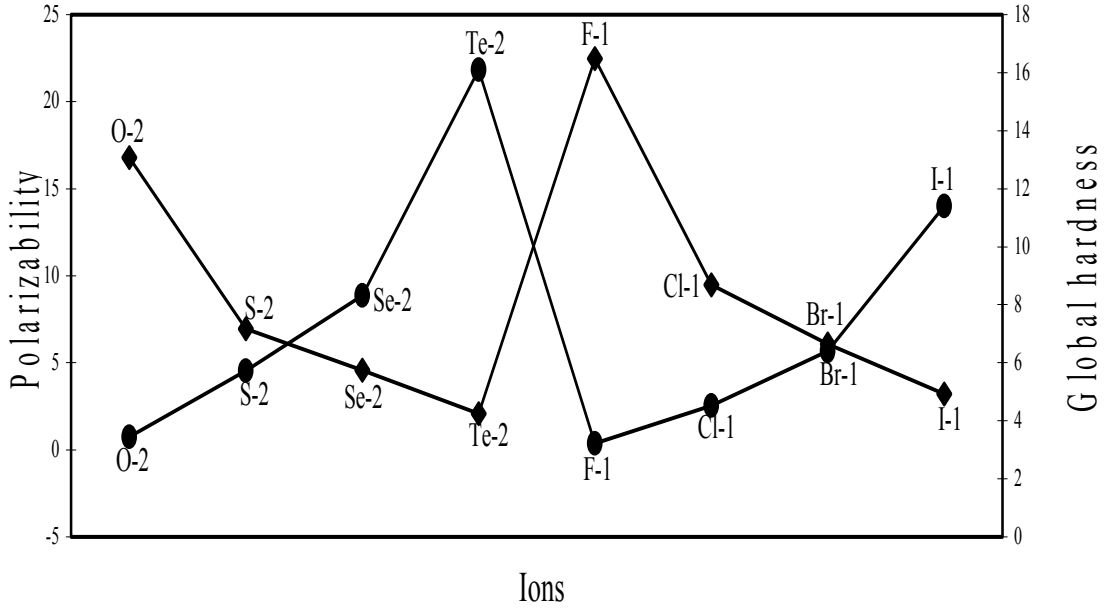

Figure 29. Plot of polarizability and global hardness of some common anions of Gr-VI and Gr-VII elements.

Table 5. Comparative study of (a) experimental (Pearson's) and (b) theoretical global hardness values of ions.

Ions	(a) Global hardness, eV	(b) Global hardness, eV	Ions	(a) Global hardness, eV	(b) Global hardness, eV
Li+1	35.12	36.69	Pt+2	8	11.31
Na+1	21.08	23.27	Hg+2	7.7	9.54
K+1	13.64	11.7	Pb+2	8.46	3.42
Rb+1	11.55	8.49	B+3	110.72	63.87
Cs+1	10.6	6.28	Al+3	45.77	30.07
Cu+1	6.28	19.7	Ga+3	17	22.72
Ag+1	6.96	11.98	In+3	13	13.82
Au+1	5.6	11.51	Tl+3	10.4	10.22
Tl+1	7.16	2.88	Sc+3	24.36	14.72
Be+2	67.84	50.28	Y+3	20.6	10.33
Mg+2	32.55	26.67	La+3	15.39	7.64
Ca+2	19.52	13.21	Ce+3	8.28	3.67
Sr+2	16.3	9.41	Lu+3	12.12	11.43
Ti+2	6.96	13.36	Ti+3	7.89	13.89
V+2	7.33	14.34	V+3	8.7	14.87
Cr+	7.23	15.32	Cr+3	9.1	15.85
Mn+2	9.02	16.31	Mn+3	8.8	16.83
Fe+2	7.24	17.29	Fe+3	12.08	17.82
Co+2	8.22	18.27	Co+3	8.9	18.8
Ni+2	8.5	19.25	Ni+3	9.9	19.78
Cu+2	8.27	20.23	Nb+3	6.6	9.04
Zn+2	10.88	21.21	Mo+3	9.6	9.64
Ge+2	9.15	5.83	Ru+3	10.7	10.83
Pd+2	6.75	11.71	Rh+3	11.2	11.43
Ag+2	6.7	12.3	Ir+3	7.9	11.11
Cd+2	10.29	12.9	Au+3	8.4	11.99

contraction in the ions of d- and f-block transition metals is correctly exhibited by the computed radii of such ions and there is good agreement between computed and experimental hardness of a number of ions. These may be used as benchmark to establish the validity of the computed theoretical radii as the representative absolute radii of the ions at their respective oxidation states.

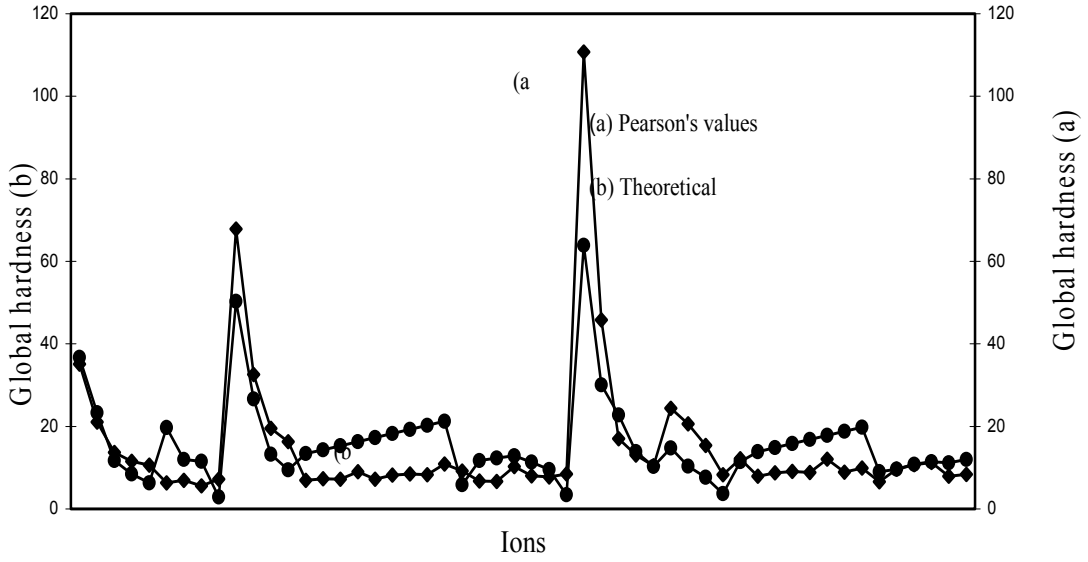

Figure 30. Plot of global hardnes of ions

Conclusion

The computed absolute sizes of ions reproduce the expected periodic behaviour in groups and periods and have a justifiable correlation with experimental radii. The expected d-block and f-block contractions of ionic sizes are nicely reproduced by the theoretical radii. It is evident from the profiles of experimental radii of the tripositive ions of the lanthanide and actinide elements that there is no distinct size contraction in the series. The profile of the experimental radii of the 3d block transition metal ions seems to exhibit that there is no expected gradual contraction in size and the variation of size as a function of atomic number is anomalous. But shielding is a physical reality and contraction of size of atoms and ions of the d-block and f- bock elements is inevitable. Thus the present study has amply demonstrated that the experimental radii of the d-block and f-block metal ions do not represent the absolute sizes of the ions rather such data create erroneous and misleading impression of the size behaviour of such series of ions. A rationale of the double hump curve of the experimental radii of 3 d-block transition metal ions is put forward in terms of the crystal field theory and Jahn-Teller distortion. The computed ionic radii are exploited to compute as many as three physico-chemical properties like diamagnetic susceptibility, polarizability and chemical hardness. Polarizability and global hardness are both radial property and inversely related to each other. The profiles of hardness and polarizability curves perfectly correlate with each other. The agreement between the experimental and theoretical global hardness computed in terms of the theoretical radii of as many as 52 ions is encouraging. The fact of good agreement between the experimental and computed global hardness of ions and correct demonstration of d-block and f-block contraction by the computed radii may be used as a benchmark to test the validity of the values of the computed theoretical radii of the ions as their representative sizes. It is demonstrated that in d- and f- block transition series, the experimental radii are absolutely wrong representation of the sizes of the ions, and the theoretical determination of the sizes of ions is

more reliable than the adopted experimental method. Thus, the theoretically computed radii of ions are visualizable size representation of ions and can be used as their absolute radii at the respective oxidation states.

Acknowledgement

One of the authors, Raka Biswas is grateful to University of Kalyani for financial assistance.

Reference:

1. Parr, R. G.; Zhou Z. *Acc. Chem. Res*. **1993**, *26*, 256 – 258.
2. Mason, J. *J. Chem. Educ*. **1988**, *65,* 17.
3. Pauling, L. *Nature of Chemical Bond and the Structure of Molecules and crystals: An Introduction to Modern Structural Chemistry,* Third Edition, Cornell University Press: Ithaka, NY, 1960.
4. (a) Slater, J. C. *J. Chem. Phys*. **1964**, *41*, 3199.
   (b) Slater, J. C. *Quantum Theory of Molecules and Solids;* McGraw-Hill: New York, Vol. 2, 1965.
5. (a) Shanon, R. D.; Prewitt, C. T. *Acta. Cryst.* **1969,** B25, 925.
   (b) Shanon, R. D.; Prewitt, C. T. *Acta. Cryst.* **1976,** A 32, 751.
6. Waber, J. T.; Cromer, D. T. *J. Chem. Phys*. **1965**, *42*, 4116.
7. Politzer, P.; Parr, R. G.; Murphy, D. R. *J. Chem. Phys*. **1983**, *79*, 3859.
8. (a) Deb, B. M.; Chattaraj, P. K. *Phys. Rev.* **1988**, *A 37*, 4030.
   (b) *ibid*, **1992**, *A 45*, 1412.
9. Deb, B. M.; Singh, R.; Sukumar, N. *J. Mol. Strut*. (*THEOCHEM*) **1992**, *259*, 121.
10. Waber, J. T.; Larson, A. C. *Rare Earth Res., Conf. Clear Water, Fla*. **1964**, *3*, 361.
11. Chattaraj, P. K. *J. Mol. Strut. (THEOCHEM)* **1995**, *331*, 267.
12. Huheey, J. E.; Keiter, E. A.; Keiter, R. L. *Inorganic Chemistry: Principles of Structure and Reactivity*, Fourth Edition, Addison-Wesley Publishing Co: New York, **1997**.
13. Sanderson, R. T. *Inorg. Chem*. **1963**, *2*, 660.
14. Sanderson, R. T. *J. Inorg. Nucl. Chem*. **1958**, *7*, 288.
15. Meek, T. L. *J. Chem. Educ*. **1995**, *72*, 17.
16. Bondi, A. *J. Phys. Chem*. **1964**, *68*, 441.
17. Rowlison, J. S. *Quart. Rev*. **1954**, *8*, 164.
18. (a) Goldschmidt, V. M. *Skrifter Norske Videnscaps – Acad. Osls* **1926**, *2*.
   (b) Goldschmidt, V. M. *Skrifter Norske Videnscaps – Acad. Osls* **1927**, *8*.
   (c) Goldschmidt, V. M. *Trans. Faraday Soc.* **1929**, *25*, 253.
   (d) Goldschmidt, V. M. *GeochemischeVerteilungsgesetze der Elemente* **1926**, *8*, 69.
   (e) Goldschmidt, V. M. *Ber* **1927**, *60*, 1263.
19. (a) Zachariasen, W. H. *Z. Cryst*. **1931,** *80*, 137.
   (b) Zachariasen, W. H. *Phys. Rev.* **1948**, *73*, 1104.
20. Bragg, W. *Phil. Mag.* **1920**, *40*, 169.
21. Nagle, J. K. *J. Am. Chem. Soc.* **1990**, *112,* 4741.
22. Dimitiieva, I. K.; Plindov, G. L. *Phys. Scr.* **1983**, *27*, 734.

23. Ghosh, D. C.; Biswas, R. *Int. J. Mol. Sci*., **2002**, *3*, 87 – 113.
24. Hertzberg, G. *Atomic Spectra and Atomic Structure*, Dover Publication: New York, 1944.
25. Atkins, P. W.; Friedman, R. S. *Molecular Quantum Mechanics*, Third Edition, Oxford University Press: Oxford, 1997.
26. Slater, J. C. *Phys. Rev*. **1930**, *36*, 57.
27. Pople, J. A.; Beveridge, D. L. *Approximate Molecular Orbital Theory*, McGraw-Hill: New York, 1970.
28. Shriver, D. F.; Atkins, P. W.; Langford, C. H. *Inorganic Chemistry*, Third Edition, Oxford University Press: Oxford, 1999.
29. Purcell, E. M. *Berkley Physics Course*, TMH Edition, Tata McGraw-Hill Publishing Company: Bombay-New Delhi, Vol. 2, 1963.
30. Pearson, R. G. *J. Am. Chem. Soc*. **1963**, *85*, 3533.
31. Pearson, R. G. *Science* **1966**, *172*, 151.
32. Brinck, T.; Murray, J. S.; Politzer, P. *J. Chem. Phys*. **1993**, *98*, 4305.
33. Hati, S.; Dutta, D. *J. Phys. Chem.* **1994**, *98*, 10451.
34. Allen, L. C. *J. Am. Chem. Soc*. **1989**, *111*, 9003.
35. Cotton, F. A.; Wilkinson, G. *Advanced Inorganic Chemistry: A Comprehensive Text*, Third Edition, John Wiley and Sons: New York, 1972.
36. Figgis, B. N. *Introduction to Ligand Fields*, Interscience: New York, 1967.
37. Carlin, R. L. *Magnetochemistry*, Springer-Verlag: New York, 1986.
38. Pearson, R. G. *Inorg. Chem*. **1988**, *27*, 734.